JOURNAL OF NATURAL PRODUCTS

Article

pubs.acs.org/jnp

Santacruzamate A, a Potent and Selective Histone Deacetylase Inhibitor from the Panamanian Marine Cyanobacterium cf. *Symploca* sp.

Christopher M. Pavlik,[†] Christina Y. B. Wong,[‡] Sophia Ononye,[†] Dioxelis D. Lopez,[‡] Niclas Engene,[§] Kerry L. McPhail,[⊥] William H. Gerwick,[§,∥] and Marcy J. Balunas*[,†,‡,§,∥]

[†]Division of Medicinal Chemistry, Department of Pharmaceutical Sciences, University of Connecticut, Storrs, Connecticut 06269, United States

[‡]Instituto de Investigaciones Científicas y Servicios de Alta Tecnología (INDICASAT), Ciudad del Saber, Clayton, Apartado Postal 0816-02852, Panama City, Panamá

[§]Center for Marine Biotechnology and Biomedicine, Scripps Institution of Oceanography and Skaggs School of Pharmacy and Pharmaceutical Sciences, University of California San Diego, La Jolla, California 92093, United States

[⊥]College of Pharmacy, Oregon State University, Corvallis, Oregon 97331, United States

[∥]Smithsonian Tropical Research Institute (STRI), Ancón, Apartado Postal 0843-03092, Panama City, Panamá

Supporting Information

ABSTRACT: A dark brown tuft-forming cyanobacterium, morphologically resembling the genus *Symploca*, was collected during an expedition to the Coiba National Park, a UNESCO World Heritage Site on the Pacific coast of Panama. Phylogenetic analysis of its 16S rRNA gene sequence indicated that it is 4.5% divergent from the type strain for *Symploca* and thus is likely a new genus. Fractionation of the crude extract led to the isolation of a new cytotoxin, designated santacruzamate A (**1**), which has several structural features in common with suberoylanilide hydroxamic acid [(**2**), SAHA, trade name Vorinostat], a clinically approved histone deacetylase (HDAC) inhibitor used to treat refractory cutaneous T-cell lymphoma. Recognition of the structural similarly of **1** and SAHA led to the characterization of santacruzamate A as a picomolar level selective inhibitor of HDAC2, a Class I HDAC, with relatively little inhibition of HDAC4 or HDAC6, both Class II HDACs. As a result, chemical syntheses of santacruzamate A as well as a structurally intriguing hybrid molecule, which blends aspects of both agents (**1** and **2**), were achieved and evaluated for their HDAC activity and specificity.

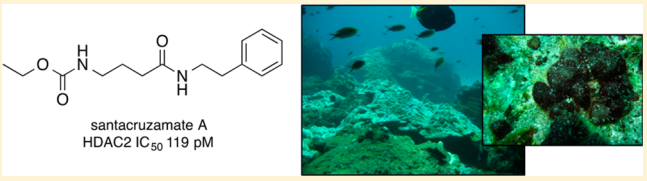

The packaging of DNA into nucleosomes is an essential process for gene transcription in eukaryotic cells, one step of which involves the winding of DNA around histone proteins to form chromatin.[1,2] Histone deacetylases (HDACs) and histone acetyltransferases (HATs) are key enzymes that regulate this process, and thus they have substantial impact on gene transcription. HDAC enzymes remove acetyl groups from lysine residues in histones, thus increasing their overall positive charge and the resulting binding affinity between histones and negatively charged DNA; this process leads to repression of gene transcription. In contrast, HATs acetylate histones, thus reducing their positive charge and allowing unwinding of the DNA that must precede gene transcription or replication.[3] HDAC inhibition prevents the removal of acetyl groups from histones, causing their accumulation in cell nuclei and resulting in several downstream effects including apoptosis, differentiation, and reduced proliferation of cancer cells.[1,3,4] In addition, HDACs have recently been shown to have a multitude of non-histone protein substrates, which may also contribute to these downstream cellular effects.[5] Such effects are of potential relevance to the treatment of several diseases such as cancer,[6,7] HIV/AIDS,[8] stroke and other neurological disorders,[9,10] and parasitic diseases.[11] The first clinically useful HDAC inhibitor, suberoylanilide hydroxamic acid (SAHA, **2**, or Vorinostat), was approved for clinical use in 2006 in patients with refractory cutaneous T-cell lymphoma.[12] In 2009, another HDAC inhibitor, romidepsin (Istodax), was also approved for cutaneous T-cell lymphoma.[13]

There are several classes of HDAC enzymes of human relevance, including Class I (HDAC 1−3, 8), Class IIa (HDAC 4, 5, 7, 9), Class IIb (HDAC 6, 10), Class III (sirtuins 1−7), and Class IV (HDAC 11).[14] The first HDAC inhibitor approved for clinical use, SAHA (**2**), is considered a pan-HDAC inhibitor with activity across several classes of HDAC enzyme. Romidepsin, the only other HDAC inhibitor currently on the market, has selectivity for Class I HDAC isozymes but is not selective within the class, exhibiting activity against HDACs 1, 2, 3, and 8.[15,16] Another marine cyanobacterial metabolite,

Received: March 8, 2013
Published: October 28, 2013

dx.doi.org/10.1021/np400198r | *J. Nat. Prod.* 2013, 76, 2026−2033

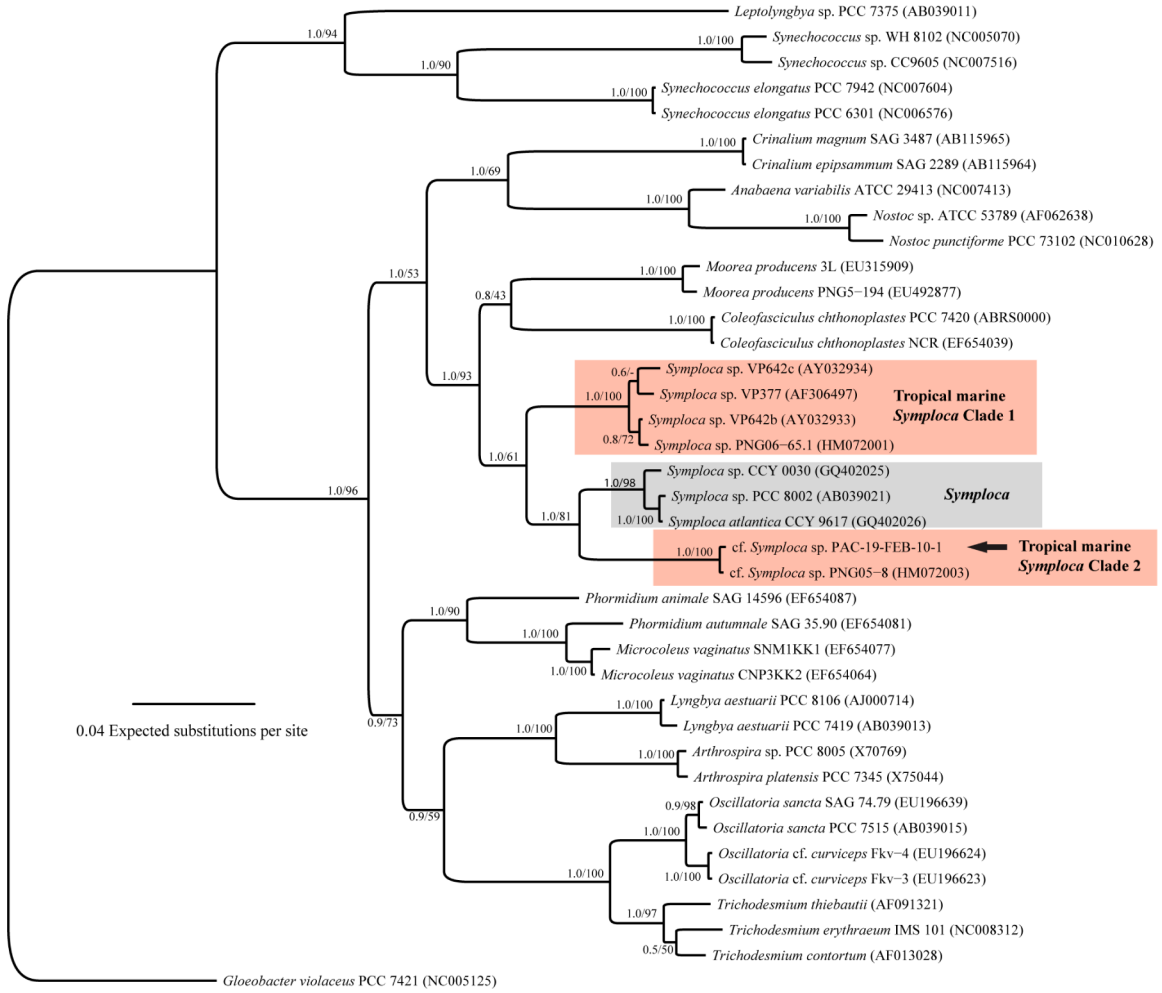

Figure 1. Molecular-phylogenetic inference of the SCA-producing strain PAC-19-FEB-10-1 (GenBank acc. no. JX458089.1, highlighted with an arrow). The closest related group is the genus *Symploca* (reference strain: PCC 8002^{T}, GenBank acc. no. AB039021) with a p-distance of 4.5% based on the SSU rRNA gene sequence divergence (gray box). The "tropical marine *Symploca*" clades are highlighted with orange boxes. The phylogram is based on SSU (16S) rRNA gene sequences using the bayesian (MrBayes) and maximum likelihood (PhyML) methods, and support values are indicated as posterior probability and bootstrap support at nodes. Specimens designated with (^{R}) represent reference-strains obtained from Bergey's Manual. The scale bar is indicated at 0.03 expected nucleotide substitution per site, corrected using the general time reversal (GTR) model.

largazole, isolated from another *Symploca* sp., has distinctive structural similarity to the active moiety of romidepsin and also selectively inhibits Class I HDACs, although does not show selectivity within the class.[16] This general lack of selectivity is believed to result in many of the undesirable side effects of these HDAC-targeting agents,[14] and recent research has focused on the search for isozyme-selective HDAC inhibitors.[17] It is hoped that agents with potent activity against one HDAC isozyme, with little or no effect on other isozymes, will result in increased clinical utility and a decreased incidence of side effects.

The Panama-based International Cooperative Biodiversity Group (ICBG) has focused on natural product drug discovery from Panamanian plants and microorganisms with a particular emphasis on the discovery of antiparasitic and anticancer lead molecules.[18−20] In this regard, our work with marine cyanobacteria has been especially productive, and a number of anticancer and antiparasitic agents have been isolated from these organisms.[21−23] In the current work, we report on the isolation of a selective HDAC inhibitor with extraordinary potency against HDAC2, a Class I HDAC enzyme. Due to the collection of the source organism from near Santa Cruz Island in Panama's Coiba National Park, a UNESCO World Heritage Site, this carbamate derivative has been named santacruzamate A (**1**).

■ RESULTS AND DISCUSSION

A dark brown cyanobacterium, morphologically resembling the genus *Symploca* (strain PAC-19-FEB-10-1, Figure S1), was collected from a coral and rock reef near Santa Cruz Island during an expedition to Coiba National Park on the Pacific coast of Panama. Microscopically, the specimen is composed of fine (9−10 μm wide) filaments with isodiametric cells covered with a barely visible sheath (Figure S1, Supporting Information).

The SSU (16S) rRNA gene sequence was obtained from the strain PAC-19-FEB-10-1 (GenBank acc. no. JX458089.1, Figure 1) and used to infer the evolution of this specimen in relation to other groups of cyanobacteria. This phylogenetic inference revealed that the closest related reference strain was *Symploca atlantica* PCC 8002^{R} (GenBank acc. no. AB039021). However, the uncorrected gene sequence divergence between this clade and the original type-strain was 4.5% over 1162 base pairs in the 16S rRNA gene. This high evolutionary divergence, in

dx.doi.org/10.1021/np400198r | *J. Nat. Prod.* 2013, 76, 2026−2033

combination with distinct biogeographic and ecological divergences, suggested that strain PAC-19-FEB-10-1 composes an independent group, distinct from the genus *Symploca*. Phylogenetically closely related to PAC-19-FEB-10-1 was the hoiamide C-producing strain PNG05-8 (GenBank acc. no. HM072003) from Papua New Guinea (p-distance = 0.1% gene sequence divergence).[24] It should be noted that there is a second lineage of "tropical marine *Symploca*" (p-distance = 5.8% gene sequence divergence from the "tropical marine *Symploca*" clade containing PAC-19-FEB-10-1 and PNG05-8), which includes the dolastatin 10-producing strain VP642b (AY032933) and the symplostatin 1-producing strain VP377 (AF306497).[25] Thus, it becomes clear that not only should "tropical marine *Symploca*" be separated from the current genus *Symploca* but also there are at least two different groups within the "tropical marine *Symploca*" that may be distinct from one another at the genus level.

A polar fraction from the initial normal-phase flash chromatography of the crude extract, fraction H (eluted with 3:1 ethyl acetate−methanol), was tested at 10 μg/mL and found to have potent activity against the malaria parasite (99.9% inhibition of parasite growth) and MCF-7 cancer cells (50% cell death indicated by negative growth, perhaps indicative of overt cytotoxicity), with no activity in leishmaniasis or Chagas' disease assays (7.9% and 9.2% inhibition, respectively). Isolation efforts continued using reversed-phase solid-phase extraction (RP-SPE) and RP high-performance liquid chromatography (HPLC) and yielded a single molecule, santacruzamate A (**1**).

By HRESIMS, a $[M + H]^+$ peak consistent with a molecular formula of $C_{15}H_{22}N_2O_3$ was obtained, indicative of six degrees of unsaturation. ^{1}H NMR spectroscopic analysis of the purified metabolite (**1**) revealed a relatively uncomplicated NMR spectrum with two amide protons (δ_H 5.92 and 4.92), five phenyl protons (δ_H 7.22−7.30), six sets of methylene protons (δ_H 4.10, 3.53, 3.18, 2.83, 2.17, and 1.80), and one methyl group (δ_H 1.23). The dispersions in chemical shift and coupling patterns helped to determine the respective linkage of these protons in four distinct spin systems (**1a**−**1d**). The most deshielded methylene signal, a quartet at δ_H 4.10, was consistent with protons attached to a carbon bearing an oxygen atom (by HSQC, δ_C 60.8) and proximal to a methyl group (for which the resonance was located by ^{1}H−^{1}H COSY at δ_H 1.23), thus defining partial structure **1a**. Two methylene groups in different spin systems had ^{1}H and ^{13}C NMR chemical shifts indicative of proximity to nitrogen atoms (δ_H 3.53 and 3.18), both of which resonated as quartets. Delineation of a second spin system (**1b**) began with the higher field of these quartets (δ_H 3.18; δ_C 40.2), which was coupled to both an amide ^{1}H singlet at δ_H 5.92 and a methylene resonance at δ_H 1.80 (CH_2-12, δ_C 26.1). The pentet splitting pattern of this latter signal suggested a third contiguous methylene group, and this was confirmed via COSY correlations between the H_2-12 and H_2-11 (δ_H 2.17; δ_C 33.7) signals. The more downfield quartet for a methylene adjacent to nitrogen (CH_2-8, δ_H 3.53 and δ_C 40.6) was proximate to another methylene (CH_2-7, δ_H 2.83, δ_C 35.7), thereby defining a $-CH_2-CH_2-$ spin system (**1c**). The fourth spin system (**1d**) was represented by three overlapping ^{1}H multiplets in the aromatic region that integrated to five protons, as is typical of a monosubstituted phenyl group (Table 1). HMBC correlations from H-7 (δ_H 2.83) and H-8 (δ_H 3.53) to C-4 (δ_C 138.9) linked partial structures **1c** and **1d** to define a phenethylamine moiety. HMBC correlations from H-8, H-11, and H-12 to an amide carbonyl at δ_C 172.5 (C-10) established the connectivity of partial structures **1b** and **1c** and further identified partial structure **1b** as a γ-aminobutyric acid residue. Finally, HMBC correlations from both H-13 and H-16 to an unusually shielded carbonyl at δ_C 157.1 (C-15) were used to connect partial structures **1a** and **1b**. The distinctive chemical shift of this C-15 carbonyl, along with the remaining atoms required by the molecular formula, was consistent with a carbamate functionality spanning these two spin systems. The final, achiral molecular structure of santacruzamate A (**1**) was thus established.

Table 1. NMR Data for Santacruzamate A (1) in $CDCl_3$

position	δ_H,[a] mult. (J in Hz)	δ_C,[b] mult.	COSY	HMBC (H→C)
1	7.23, m	126.5, CH	2, 6	3, 5
2	7.30, m	128.8, CH	1, 3	4, 6
3	7.22, m	128.6, CH	2	1, 5, 7
4		138.9, qC		
5	7.22, m	128.6, CH	6	1, 3, 7
6	7.30, m	128.8, CH	1, 5	2, 4
7	2.83, t (6.8)	35.7, CH_2	8	3, 4, 5, 8
8	3.53, q (6.8)	40.6, CH_2	7, 9	4, 7, 10
9	5.92, br s		8	
10		172.5, qC		
11	2.17, t (6.9)	33.7, CH_2	12	10, 12, 13
12	1.80, pentet (6.8)	26.1, CH_2	11, 13	10, 11, 13
13	3.18, q (5.9)	40.2, CH_2	12, 14	11, 12, 15
14	4.92, br s		13	
15		157.1, qC		
16	4.10, q (6.9)	60.8, CH_2	17	15, 17
17	1.23, t (7.3)	14.7, CH_3	16	16

[a]Measured at 400 MHz. [b]Measured at 100 MHz.

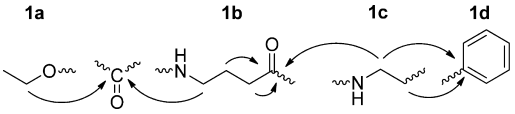

Figure 2. Partial structures of santcruzamate **1a**-**1d**, and their connectivity by HMBC (arrows).

Santacruzamate A (**1**) has several structural features in common with SAHA (**2**), a clinically approved histone deacetylase inhibitor used to treat refractory cutaneous T-cell lymphoma.[12] The target of SAHA includes all isozyme subtypes of histone deacetylases, the consequence of which is to upregulate the transcription of cell cycle regulators, nuclear transcription factors, and pro-apoptotic genes, thus bringing about an overall antineoplastic effect. Some structural similarity to **1** can also be seen with two other marine natural products: psammaplin H (**4**), a moderate HDAC inhibitor isolated from a marine sponge with which santacruzamate shares the ethyl carbamate functionality,[26] and grenadamide (**5**) from a marine cyanobacterium, with which santacruzamate shares the phenethylamine moiety and which has shown activity in a central nervous system (CNS) assay.[27]

SAHA (**2**) binds to HDAC enzymes such that the phenyl cap sits above the enzyme pocket into which the aliphatic chain inserts, positioning the hydroxamic acid adjacent to the enzymatic zinc at the distal end of the pocket.[2] Given this binding mechanism and the structural similarity between **1** and SAHA, it was hypothesized that santacruzamate A might also be an HDAC inhibitor. Consequently, the chemical syntheses of

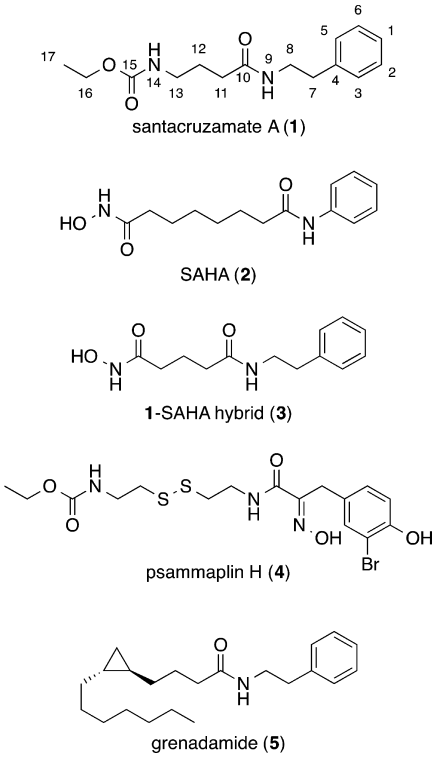

compound **1** and a structurally intriguing hybrid structure blending aspects of both **1** and SAHA were undertaken (Figure 3). In brief, GABA was converted to the carbamate intermediate 4-((ethoxycarbonyl)amino)butanoic acid via reaction with K_2CO_3 and ethyl chloroformate in water (76% yield).[28] This intermediate was coupled to phenethylamine using *N*-(3-dimethylaminopropyl)-*N*′-ethylcarbodiimide hydrochloride (EDC-HCl), triethylamine (TEA), and catalytic 4-(dimethylamino)pyridine (DMAP) to yield santacruzamate A (**1**, 92% yield, overall yield 70%). To create an **1**−SAHA hybrid structure (**3**, Figure 3B), phenethylamine was coupled to monomethyl glutarate via the peptide coupling described above (88% yield), and then this intermediate was converted to the hydroxamic acid via standard literature procedures using hydroxylamine hydrochloride and KOH in methanol to afford compound **3** (90% yield, overall yield 79%).[29]

The synthetic products **1** and **3**, as well as the original natural product santacruzamate A (**1**), were all evaluated for isozyme-selective inhibition of HDAC2, a Class I HDAC, and HDAC4, a Class IIa HDAC. Initial results revealed that compounds **1** and **3** at 1 μM selectively inhibited HDAC2 with relatively little inhibition of HDAC4 (data not shown). In contrast, at 1 μM SAHA completely inhibited both Class I and II HDAC enzymes. On the basis of these promising results, IC_{50} values for the natural product **1**, synthetic **1**, the **1**−SAHA hybrid, and authentic SAHA were determined using HDAC2, HDAC4, and HDAC6, a Class IIb HDAC. Against HDAC2, SAHA (**2**) showed an IC_{50} of 85.8 nM, whereas natural and synthetic **1** yielded values of 119 and 112 pM, respectively. Thus, **1** is over 700-fold more potent for HDAC2 than the clinically useful drug SAHA. The **1**−SAHA hybrid (**3**) was of diminished activity compared to **1**, with an IC_{50} value of 3.5 nM against HDAC2. Intriguingly, both samples of **1** and the **1**−SAHA (**3**) hybrid were found to have IC_{50} values of more than 1 μM against HDAC4, indicating a strong selectivity for Class I HDAC inhibition. Santacruzamate A (**1**) and **1**−SAHA (**3**) were further tested against HDAC6 and found to have IC_{50} values of 433.5 and 385.8 nM, respectively, while SAHA (**2**) showed limited selectivity, with an IC_{50} of 38.9 nM (Table 2). The combination of picomolar potency and the greater than 3500-fold selectivity for Class I HDACs makes santacruzamate A (**1**) an exciting lead compound.

Subsequently, the natural product **1** and synthetic compounds were tested for cytotoxicity to HCT-116 colon carcinoma cells, HuT-78 cutaneous T-cell lymphoma cells, and human dermal fibroblast (hDF) cells. SAHA (**2**) was used as the positive control and showed a GI_{50} value of 0.4 μM in HCT-116 cells, 3.0 μM for HuT-78 cells, and 6.1 μM in hDF cells (Table 2). **1**−SAHA was slightly less potent in HCT-116 cells (GI_{50} of 2.3 μM) but of somewhat greater potency against HuT-78 cells (GI_{50} 0.7 μM), with no activity using hDF cells (GI_{50} >100 μM). The natural and synthetic **1** were found to be of only moderate potency in HCT-116 cells, with GI_{50} values of 29.4 and 28.3 μM, respectively. However, both potently inhibited the growth of HuT-78 cells with GI_{50} values of 1.4 and 1.3 μM, respectively, and neither exhibited activity against hDF cells (GI_{50} >100 μM). The 20-fold differential activity of **1** found against HCT-116 and HuT-78 cells poses several interesting avenues for further research, including determining if these cellular responses are due to HDAC inhibition or to other cellular effects. Additional testing using the National Cancer Institute (NCI) in vitro panel of 60 cancer cell lines is ongoing, and studies to investigate the levels of cellular acetylation are planned.

Given the remarkable potency and selective HDAC inhibition of santacruzamate A (**1**), it is of interest to create structural analogues so as to enhance cellular activity as well as

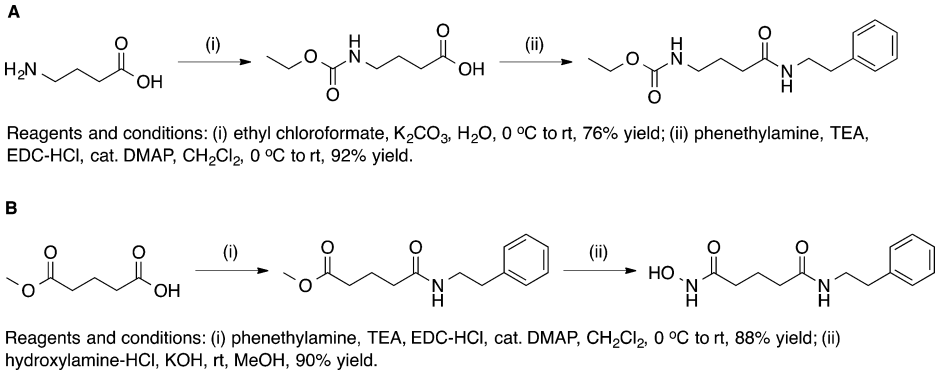

Figure 3. Synthetic schemes for preparation of (A) SCA (**1**) and (B) the SCA−SAHA hybrid (**3**).

dx.doi.org/10.1021/np400198r | *J. Nat. Prod.* 2013, 76, 2026−2033

Table 2. Biological Activity of Santacruzamate (1) and Synthetic Compounds against Class I and Class II HDACs Using HDAC2, HDAC4, and HDAC6 as Well as in Cellular Cytotoxicity Testing Using HCT-116 Colon Cancer, HuT-78 Cutaneous T-Cell Lymphoma, and Human Dermal Fibroblast (hDF) Cells

	HDAC2	HDAC4	HDAC6		HCT116	Hut-78	hDF
	IC_{50} (nM)	IC_{50} (nM)	IC_{50} (nM)	SI[a]	GI_{50} (μM)	GI_{50} (μM)	GI_{50} (μM)
1 (natural product)	0.119	>1000	434	3647	29.4	1.4	>100
1 (synthetic)	0.112	>1000	433	3866	28.3	1.3	>100
3	3.5	>1000	386	110	2.3	0.7	>100
2 (positive control)	85.8	n.d.	38.9	0.33	0.4	3.0	6.1

[a]SI = selectivity index calculated as HDAC6/HDAC2; n.d. = no data.

to determine its mechanism of enzymatic inhibition. Due to its small and linear peptide-type structure, **1** is amenable to synthetic modifications to explore structure−activity relationships, especially considering the structural similarities to known HDAC-active compounds. Further modification of **1** could result in the design of more potent analogues with the potential for preclinical development and provide opportunities for facile chemical scale-up. Indeed, the robust synthesis reported herein has been employed to produce a focused library of additional analogues, the biological properties of which are currently under evaluation and will be reported in due course.

EXPERIMENTAL SECTION

General Experimental Procedures. Melting points were collected on a Mel-Temp digital melting point apparatus. IR spectra were recorded on a Shimadzu FT-IR 8400 spectrometer. NMR spectra for the natural product SCA (**1**) were obtained on a JEOL Eclipse 400 MHz spectrometer and referenced to TMS. All other NMR spectra were recorded on a Brüker Avance 500 MHz spectrometer (500.13 MHz ^{1}H, 125.65 MHz ^{13}C), with chemical shifts given in ppm downfield from TMS. LC-MS data were collected on an Agilent ESI single quadrupole mass spectrometer coupled to an Agilent HPLC system with a G1311 quaternary pump, G1322 degasser, and a G1315 diode array detector using an Eclipse XDB-C_{18} (4.6 × 150 mm, 5 μm) RP-HPLC column. High-resolution mass spectrometric data (HRMS) were collected on a Micromass VB-QTOF tandem mass spectrometer. HPLC purifications of natural product isolates were carried out on a Merck Hitachi LaChrom HPLC system with an L-7100 pump, an L-7614 degasser, and an L-7455 diode array detector using a Prontosil-120 C_{18} (4.6 × 250 mm, 5 μM) RP-HPLC column, with the solvent systems as indicated below. All chemicals were used as received from Sigma-Aldrich or Acros without further purification. Hexanes, tetrahydrofuran (THF), diethyl ether (Et_2O), and dichloromethane (CH_2Cl_2) were used directly from a Baker Cycle-tainer system. All glassware was flame-dried under a vacuum, and all reactions were performed under an argon atmosphere, unless otherwise noted. Thin-layer chromatography was carried out on Fluka glass-backed TLC plates with a fluorescent indicator and 0.2 mm silica gel layer thickness, and *p*-anisaldehyde was used as a developing agent. Column chromatography was done using 60 Å porosity, 32−63 μm silica gel. Structural integrity and purity of the test compounds were determined by the composite of ^{1}H and ^{13}C NMR spectroscopy, melting point range, LC-MS, and HRMS, and compounds were found to be >95% pure.

Collection, Extraction, and Isolation. A cyanobacterium morphologically resembling the genus *Symploca* (Figure S1) was collected in March 2007 by hand using SCUBA at depths of 30−45 feet. The collection site was a coral and rock reef (Figure 1A) in Coiba National Park (7°37.980 N, 81°47.091 W) in Veraguas, Panama. After straining through a mesh bag to remove excess seawater, the sample was stored in 1:1 EtOH−seawater at −20 °C. The voucher specimen, number PAC-03/03/2007-1, is deposited at Scripps Institution of Oceanography, UCSD (San Diego, CA, USA). The sample (221.5 g dry weight) was thawed and extracted exhaustively with 2:1 CH_2Cl_2−MeOH. After solvent evaporation, 2.1 g of a crude organic extract was obtained. The extract was fractionated using flash Si gel column chromatography (Aldrich, Si gel 60, 230−400 mesh, 40 × 180 mm) using 300 mL each of 100% hexanes (A), 9:1 hexanes−EtOAc (B), 4:1 hexanes−EtOAc (C), 3:2 hexanes−EtOAc (D), 2:3 hexanes−EtOAc (E), 1:4 hexanes−EtOAc (F), 100% EtOAc (G), 3:1 EtOAc−MeOH (H), and 100% MeOH (I). Fraction H exhibited strong antimalarial activity (99.9% inhibition of parasite growth at 10 μg/mL) and was subjected to further fractionation using a Burdick & Jackson C_{18} RP-SPE cartridge with a MeOH−H_2O solvent gradient (1:1, 3:2, 7:3, 4:1 MeOH−EtOAc, 100% MeOH, 100% EtOAc). The fraction eluting with 1:1 MeOH−H_2O was subjected to RP-HPLC purification (55% MeOH−45% H_2O, 1.0 mL/min) to yield santacruzamate A (**1**, 4.0 mg, t_R 10.9 min, 0.19% of extract).

Santacruzamate A (1): white, amorphous solid; mp 112−113 °C; IR ν_{max} (film) 3345, 3288, 1703, 1699, 1655, 1543, 1538, 1446, 1307, 1285, 1249, 1223, 1139, 1050, 1031 cm^{-1}; ^{1}H and ^{13}C NMR data ($CDCl_3$, 400 and 100 MHz, respectively), see Table 1; ESIMS *m*/*z* (%) 301.1 (8, $[M + Na]^+$), 280.2 (25), 279.3 (100, $[M + H]^+$); HRESIMS $[M + H]^+$ *m*/*z* 279.1721 (calcd for $C_{15}H_{23}N_2O_3$, 279.1709).

Morphological Characterization. Morphological characterization was performed using an Olympus IX51 epifluorescent microscope (1000×) equipped with an Olympus U-CMAD3 camera. Measurements were provided as means ± standard deviation. The filament means were the average of three filament measurements, and cell measurements the average of 10 adjacent cells in each of three filaments. Morphological comparison and putative taxonomic identification of the cyanobacterial specimen were performed in accordance with modern classification systems.[30,31]

Gene Sequencing. Cyanobacterial specimens were preserved for genetic analysis both as live material and in 10 mL RNAlater (Ambion). Algal biomass (~50 mg) was partly cleaned under an Olympus VMZ dissecting microscope. Genomic DNA was extracted using the Wizard Genomic DNA purification kit (Promega) following the manufacturer's specifications. DNA concentration and purity were measured on a DU 800 spectrophotometer (Beckman Coulter). The 16S rRNA genes were PCR-amplified from isolated DNA using the general primer set 106F and 1509R,[32] while subsequent PCR reactions were performed using the modified lineage-specific primers. The PCR reaction volumes were 25 μL containing 0.5 μL (~50 ng) of DNA, 2.5 μL of 10 × PfuUltra IV reaction buffer, 0.5 μL (25 mM) of dNTP mix, 0.5 μL of each primer (10 μM), 0.5 μL of PfuUltra IV fusion HS DNA polymerase, and 20.5 μL of dH_2O. The PCR reactions were performed with an Eppendorf Mastercycler gradient as follows: initial denaturation for 2 min at 95 °C, 25 cycles of amplification, followed by 20 s at 95 °C, 20 s at 55 °C, and 1.5 min at 72 °C, and final elongation for 3 min at 72 °C. PCR products were analyzed on agarose gel (1%) in SB buffer and visualized by EtBr staining. The PCR products were purified using a MinElute PCR purification kit (Qiagen) before subcloning using the Zero Blunt TOPO PCR cloning kit (Invitrogen), following the manufacturer's specifications. Plasmid DNA was isolated using the QIAprep Spin Miniprep kit (Qiagen) and sequenced with M13 primers. The 16S rRNA gene sequence is available in the DDBJ/EMBL/GenBank databases under accession number JX458089-1.

Phylogenetic Inference. The 16S rRNA gene sequence of PAC-19-FEB-10-1 was aligned with evolutionarily informative cyanobacteria using the L-INS-I algorithm in MAFFT 6.717[33] and refined using the SSU secondary structure model for *Escherichia coli* J01695[34] without data exclusion. The best-fitting nucleotide substitution model optimized by maximum likelihood (ML) was selected using corrected Akaike/Bayesian information criterion (AIC_C/BIC) in jModeltest 0.1.1.[35] The evolutionary histories of the cyanobacterial genes were inferred using ML and Bayesian inference (BI) algorithms. The ML inference was performed using PhyML[36] for the GTR+I+G model assuming heterogeneous substitution rates and gamma substitution of variable sites (proportion of invariable sites (pINV) = 0.495, shape parameter (α) = 0.452, number of rate categories = 4) with 1000 bootstrap-replicates. The Bayesian inference was conducted using MrBayes 3.1[37] with four Metropolis-coupled MCMC chains (one cold and three heated) run for 1 000 000 generations. The first 25% were discarded as burn-in, and the following data set was sampled with a frequency of every 100 generations.

Synthesis of Santacruzamate A (1) and 1−SAHA Hybrid (3). Full experiemental details are provided below for synthetic intermediates and products of **1** and the **1**−SAHA hybrid (**3**).

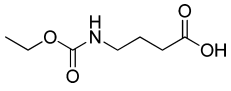

4-[(Ethoxycarbonyl)amino]butanoic Acid. γ-Aminobutyric acid (0.50 g, 4.85 mmol) was dissolved in H_2O (7 mL). Once dissolved, K_2CO_3 (1.74 g, 12.6 mmol) was added, and the resulting solution was cooled to 0 °C. Ethyl chloroformate (0.63 mL, 6.31 mmol) was added dropwise, and the solution was stirred at 0 °C for 2 h and then stirred overnight at rt. The reaction mixture was then diluted with H_2O (20 mL) and extracted with EtOAc (3 × 10 mL). The aqueous phase was acidified to pH 2 with cold concentrated HCl and extracted with EtOAc (3 × 20 mL). The EtOAc partitions were dried over Na_2SO_4 and concentrated to reveal a white solid, which was recrystallized from cold hexanes to yield long white crystals (0.645 g, 3.68 mmol, 76% yield): mp 44.1−45.0 °C; ^{1}H NMR (500 MHz, methanol-d_4) δ 4.12 (2H, q, J = 6.94 Hz), 2.85 (2H, t, J = 6.94 Hz), 2.20 (2H, t, J = 6.94 Hz), 1.82 (2H, pentet, J = 6.78 Hz), 1.25 (3H, t, J = 7.25 Hz); ^{13}C NMR (methanol-d_4) δ 177.3, 157.1, 60.8, 40.6, 35.7, 26.1, 14.7.

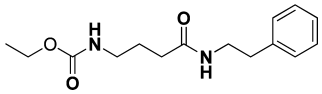

Ethyl 3-(Phenethylcarbamoyl)propylcarbamate (santacruzamate A, 1). 4-[(Ethoxycarbonyl)amino]butanoic acid (0.40 g, 2.28 mmol) was dissolved in CH_2Cl_2 (7 mL) and cooled to 0 °C. Phenethylamine (0.327 mL, 2.60 mmol) and triethylamine (0.64 mL, 4.56 mmol) were added to the solution followed by 1-ethyl-3-(3-dimethylaminopropyl)carbodiimide hydrochloride (0.50 g, 2.60 mmol) in one portion. 4-Dimethylaminopyridine (cat.) was added, and the solution was stirred at 0 °C for 60 min, then overnight at rt. The resulting solution was diluted with additional CH_2Cl_2 (20 mL) and washed sequentially with 10 mL of each of the following: 1.0 M HCl, saturated $NaHCO_3$, H_2O, brine. The organic layer was dried over Na_2SO_4 and concentrated to give a residue that was recrystallized by trituration with hexanes. Upon cooling to 0 °C, the solution was filtered to yield **1**, which was obtained as a white solid (0.58 g, 92% yield): mp 112−113 °C; IR ν_{max} (film) 3345, 3288, 1703, 1699, 1655, 1543, 1538, 1446, 1307, 1285, 1249, 1223, 1139, 1050, 1031 cm^{-1}; ^{1}H NMR (500 MHz, $CDCl_3$) δ 7.30−7.36 (2H, m), 7.20−7.28 (3H, m), 5.96 (1H, br s), 4.96 (1H, br s), 4.12 (2H, q, J = 6.94 Hz), 3.55 (2H, q, J = 6.73 Hz), 3.20 (2H, q, J = 5.88 Hz), 2.85 (2H, t, J = 6.94 Hz), 2.20 (2H, t, J = 6.94 Hz), 1.82 (2H, pentet, J = 6.78 Hz), 1.25 (3H, t, J = 7.25 Hz); ^{13}C NMR (126 MHz, $CDCl_3$) δ 172.5, 157.1, 138.9, 128.8, 128.6, 126.5, 60.8, 40.6, 40.2, 35.7, 33.7, 26.1, 14.7; ESIMS m/z (%) 301.1 (8, $[M + Na]^+$), 280.2 (25) 279.3 (100, $[M + H]^+$); HRESIMS $[M + H]^+$ m/z 279.1726 (calcd for $C_{15}H_{23}N_2O_3$, 279.1709).

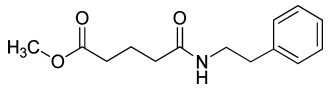

Methyl 4-(Phenethylcarbamoyl)butanoate. Monomethyl glutarate (1.00 g, 6.84 mmol) was taken up in CH_2Cl_2 (12 mL) and cooled to 0 °C. Phenethylamine (0.95 mL, 7.53 mmol) and triethylamine (1.91 mL, 13.68 mmol) were added to the solution followed by 1-ethyl-3-(3-dimethylaminopropyl)carbodiimide hydrochloride (1.44 g, 7.53 mmol) in one portion. 4-Dimethylaminopyridine (cat.) was added, and the solution was stirred overnight at rt. The resulting mixture was diluted with additional CH_2Cl_2 (20 mL) and washed sequentially with 20 mL of each of the following: 1.0 M HCl, saturated $NaHCO_3$, H_2O, brine. The organic phase was then passed through Celite, dried over Na_2SO_4, and concentrated to yield 4-(phenethylcarbamoyl)butanoate (1.50 g, 6.02 mmol, 88% yield) as a clear crystalline solid: mp 58.3−59.8 °C; ^{1}H NMR (500 MHz, $CDCl_3$) δ 7.30−7.36 (2H, m), 7.19−7.28 (3H, m), 5.57 (1H, br s), 3.68 (3H, s), 3.52−3.57 (2H, m), 2.84 (2H, t, J = 6.94 Hz), 2.37 (2H, t, J = 7.25 Hz), 2.18−2.23 (2H, m), 1.95 (2H, pentet, J = 7.25 Hz); ^{13}C NMR (126 MHz, $CDCl_3$) δ 173.6, 172.0, 138.8, 128.6, 128.7, 126.5, 51.6, 40.5, 35.7, 35.5, 33.0, 20.8; HRESIMS $[M + H]^+$ m/z 250.1431 (calcd for $C_{14}H_{20}NO_3$, 250.1443).

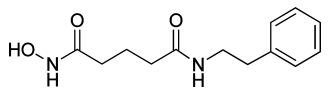

N^1-Hydroxy-N^5-phenethylglutaramide (1−SAHA hybrid, 3). Hydroxylamine hydrochloride (5.55 g, 79.8 mmol) in methanol (150 mL) was mixed with KOH (4.48 g, 79.8 mmol) at 40 °C in methanol (22 mL), cooled to 0 °C, and filtered. The butyric acid methyl ester (1.08 g, 4.43 mmol) was then added to the filtrate followed by addition (over 30 min) of KOH (0.36 g, 6.49 mmol). The mixture was stirred at rt overnight. The resulting solution was concentrated and resuspended in 50 mL of ice cold H_2O, and the pH was adjusted to 7.0 using acetic acid. The solution was cooled overnight at 0 °C to yield **3** (0.98 g, 4.13 mmol, 90%) as a white, crystalline solid: mp 106−107 °C; IR ν_{max} (film) 3302, 3177, 2920, 2360, 2340, 1623, 1617, 1565, 1458, 1419, 1195, 1033, 940 cm^{-1}; ^{1}H NMR (500 MHz, methanol-d_4) δ 7.30−7.37 (2H, m), 5.52 (1H, br s), 3.51−3.58 (2H, m), 2.84 (2H, t, J = 6.94 Hz), 2.37 (2H, t, J = 7.25 Hz), 2.21 (2H, t, J = 7.41 Hz), 1.96 (2H, pentet, J = 7.25 Hz); ^{13}C NMR (126 MHz, methanol-d_4) δ 173.8, 170.8, 139.1, 128.4, 128.1, 125.9, 40.6, 35.1, 34.8, 31.6, 21.7; ESIMS m/z (%) 273.1 (8, $[M + Na]^+$), 252.1 (15), 251.1 (100, $[M + H]^+$), 218.2 (10); HRESIMS $[M + H]^+$ m/z 251.1370 (calcd for $C_{13}H_{19}N_2O_3$, 251.1396).

Biological Assays. All assays were run using established protocols or following kit directions. Brief experimental details are provided below.

Plasmodium falciparum (Malaria) Assay. *P. falciparum* malaria parasites were maintained and assayed in human erythrocytes, from a chloroquine-resistant *P. falciparum* strain (Indochina W2).[38] A modified Trager and Jensen method was used to maintain cultures in vitro in type O+ human erythrocytes. The bioassay involved the use of synchronized ring form parasites that were incubated with extracts, fractions, compounds, or controls (chloroquine was used as a positive control) for 48 h within a humidified, airtight container, flushed with a specialized gas mixture (5% CO_2, 5% O_2, and 90% N_2). Parasite percent growth (%G) was measured using an aliquot of culture medium transferred to a new plate, permeabilized with Triton X, and treated with PicoGreen. PicoGreen is a fluorescent nucleic acid stain for quantitating double-stranded DNA. The bioassay measured parasite %G by determining the quantity of PicoGreen intercalated into intact parasitic DNA (erythrocytes are anucleate and so do not absorb PicoGreen).

Leishmania donovani (Leishmaniasis) Assay. A WHO reference strain of *L. donovani* (LD-1S/MHOM/SD/00-strain 1S) was maintained in the promastigote stage using established protocols.[39] The bioassay used the amastigote form of *L. donovani*, which is induced using a change in pH, temperature, and medium. To avoid

dx.doi.org/10.1021/np400198r | J. Nat. Prod. 2013, 76, 2026−2033

possible interference of the host cell, extracellular amastigotes were used 96 h after conditions were changed. Extracts, fractions, compounds, or controls (amphotericin B was used as positive control) were combined with the axenic amastigotes for 72 h, after which time parasite %G was measured using PicoGreen fluorescence.

Trypanosoma cruzi (Chagas' Disease) Assay. Extracts, fractions, compounds, or controls (nifurtimox was the positive control) were tested using a transgenic, β-galactosidase-expressing, *T. cruzi* (Tulahuen strain, clone C4).[40] African green monkey kidney (Vero) cells were plated with trypomastigotes added after 24 h. After invasion of *T. cruzi* parasites into the Vero cells (48 h), the parasites changed to the amastigote form, at which time extracts, fractions, compounds, or controls were added. Inhibition of parasite growth (%IG) was measured colorimetrically 5 days later, based on the cleavage of chlorophenol red-β-D-galactopyranoside by the parasite-expressed β-galactosidase.

HDAC Enzyme Assay. Three HDAC isozymes [HDAC2 (Class I), HDAC4 (Class Ia), and HDAC6 (Class IIb)] were utilized to determine percent inhibition and IC_{50} values of santacruzamate A (**1**) and the **1**−SAHA hybrid (**3**), using commercially available human recombinant enzyme (BPS Bioscience) and fluorogenic HDAC assay kits (HDAC2 kit from Active Motif; HDAC4 and HDAC6 kits from BPS Bioscience). SAHA (**2**, Vorinostat; Sigma Aldrich, St. Louis, MO, USA) served as a control for the enzyme inhibition assay. Assay data were subjected to nonlinear regression analysis (GraphPad Software, Inc., La Jolla, CA, USA). Enzyme inhibition assays were performed with varying concentrations of **1**, **2**, or **3**. Briefly, components were added sequentially to a black, flat-bottom 96-well microtiter plate (Sigma-Aldrich) as described by the manufacturer's protocol, and the reaction mixture was incubated for 30 min at 37 °C. The potent HDAC inhibitor trichostatin A (included in the assay kit) was added to the bifunctional HDAC assay developer at a final reaction concentration of 1 μM to stop deacetylation and initiate the release of the fluorophore. The reaction mixture was further incubated at room temperature for 15 min. Fluorescence was measured on a Spectra Max Gemini XPS (Molecular Devices, Sunnyvale, CA, USA) using an excitation wavelength of 360 nm and a detection wavelength of 460 nm. Inhibition assays were used to determine the half-maximal inhibitory concentration, IC_{50}, in HDAC2.

Cell Cytotoxicity Assay. Antiproliferative activity was determined using a standard MTS−PMS assay [3-(4,5-dimethylthiazol-2-yl)-5-(3-carboxymethoxyphenyl)-2-(4-sulfophenyl)-2*H*-tetrazolium, MTS; phenazine methosulfate, PMS].

Human colon cancer cells (HCT-116) were obtained from the American Type Culture Collection (ATCC, Manassas, VA, USA) and cultivated according to the supplier's instructions using McCoy's 5A medium supplemented with 10% fetal bovine serum (FBS), 1% penicillin/streptomycin, and 1% nonessential amino acids. Upon subconfluent growth, cells were seeded in a 96-well plate at 5000 cells per well. Before treatment, the plates were incubated at 37 °C, 5% CO_2 for 24 h. Treatment with test compounds was carried out in triplicate wells for 96 h using SAHA (**3**) as a positive control.

Human cutaneous T lymphocyte (HuT-78) cells were obtained from ATCC and cultivated according to the supplier's instructions using Iscove's modified Dulbecco's medium supplemented with 20% FBS, 1% penicillin/streptomycin, and 1% L-glutamine. Cells were seeded at log growth phase at 50 000 cells per well. Plates were incubated at 37 °C, 5% CO_2 for 4 h, treated with compounds in triplicate, and incubated for 72 h using SAHA (**3**) as a positive control.

Human dermal fibroblast (hDF) cells were cultivated using Dulbecco's modified Eagle medium F-12 medium supplemented with 40% FBS and 1% penicillin/streptomycin. Cells were seeded at 5000 cells per well and incubated at 37 °C, 5% CO_2 for 24 h (adherent cells). Treatment with compounds was carried out in triplicate for 72 h using SAHA (**3**) as a positive control.

IC_{50} cell cytotoxicity values were determined by varying concentrations of all compounds, and assay data were subjected to nonlinear regression analysis (GraphPad Software, Inc., La Jolla, CA, USA).

■ ASSOCIATED CONTENT

Supporting Information

Macroscopic and microscopic images of the santacruzamate A-producing organism, NMR spectra for santacruzamate A (**1**) including ^1H, ^{13}C, COSY, HSQC, and HMBC, and ^1H and ^{13}C NMR spectra for synthetic **1** and the **1**−SAHA hybrid (**3**). This material is available free of charge via the Internet at http://pubs.acs.org.

■ AUTHOR INFORMATION

Corresponding Author

*Tel: +1-860-486-3051. Fax: +1-860-486-6857. E-mail: marcy.balunas@uconn.edu.

Notes

The authors declare no competing financial interest.

■ ACKNOWLEDGMENTS

Funding for this research was provided by a Fogarty International Center (FIC) International Cooperative Biodiversity Group (ICBG) grant based in Panama (U01 TW006634) and by an FIC International Research Scientist Development Award (IRSDA) (K01 TW008002). We thank M. K. Hadden (UConn) for access to mammalian cell culture facilities, A. Anderson (UConn) for initial HDAC results, D. Wright (UConn) for dry solvents, and T. Rasmussen (UConn) for hDF cells. We are grateful to the Autoridad Nacional del Ambiente (ANAM) for providing access to biological samples in Panama and to C. Thornburg for assistance in collection of the sample.

■ REFERENCES

(1) Wang, H.; Dymock, B. W. *Expert Opin. Ther. Pat.* **2009**, *19*, 1727−1757.
(2) Marks, P.; Rifkind, R. A.; Richon, V. M.; Breslow, R.; Miller, T.; Kelly, W. K. *Nat. Rev. Cancer* **2001**, *1*, 194−202.
(3) Johnstone, R. W. *Nat. Rev. Drug Discovery* **2002**, *1*, 287−299.
(4) Khan, O.; La Thangue, N. B. *Immunol. Cell Biol.* **2012**, *90*, 85−94.
(5) Smith, K. T.; Workman, J. L. *Nat. Biotechnol.* **2009**, *27*, 917−919.
(6) Giannini, G.; Cabri, W.; Fattorusso, C.; Rodriquez, M. *Future Med. Chem.* **2012**, *4*, 1439−1460.
(7) Gryder, B. E.; Sodji, Q. H.; Oyelere, A. K. *Future Med. Chem.* **2012**, *4*, 505−524.
(8) Wightman, F.; Ellenberg, P.; Churchill, M.; Lewin, S. R. *Immunol. Cell Biol.* **2012**, *90*, 47−54.
(9) Faraco, G.; Cavone, L.; Chiarugi, A. *Mol. Med.* **2011**, *17*, 442−447.
(10) Lv, L.; Tang, Y. P.; Han, X.; Wang, X.; Dong, Q. *Cent. Nerv. Syst. Agents Med. Chem.* **2011**, *11*, 138−149.
(11) Andrews, K. T.; Haque, A.; Jones, M. K. *Immunol. Cell Biol.* **2012**, *90*, 66−77.
(12) Marks, P. A. *Oncogene* **2007**, *26*, 1351−1356.
(13) VanderMolen, K. M.; McCulloch, W.; Pearce, C. J.; Oberlies, N. H. *J. Antibiot.* **2011**, *64*, 525−531.
(14) Ononye, S. N.; van Heyst, M.; Falcone, E. M.; Anderson, A. C.; Wright, D. L. *Pharm. Pat. Analyst* **2012**, *1*, 207−221.
(15) Bertino, E. M.; Otterson, G. A. *Expert Opin. Investig. Drugs* **2011**, *20*, 1151−1158.
(16) Hong, J.; Luesch, H. *Nat. Prod. Rep.* **2012**, *29*, 449−456.
(17) Pan, H.; Cao, J.; Xu, W. *Anticancer Agents Med. Chem.* **2012**, *12*, 247−270.
(18) Kursar, T. A.; Caballero-George, C. C.; Capson, T. L.; Cubilla-Rios, L.; Gerwick, W. H.; Gupta, M. P.; Ibañez, A.; Linington, R. G.; McPhail, K. L.; Ortega-Barría, E.; Romero, L. I.; Solis, P. N.; Coley, P. D. *Bioscience* **2006**, *56*, 1005−1012.

(19) Kursar, T. A.; Capson, T. L.; Coley, P. D.; Corley, D. G.; Gupta, M. B.; Harrison, L. A.; Ortega-Barria, E.; Windsor, D. M. *Pharm. Biol.* **1999**, *37* (Suppl.), 114−126.
(20) Capson, T. L.; Coley, P. D.; Kursar, T. A. *Nat. Biotechnol.* **1996**, *14*, 1200−1202.
(21) Balunas, M. J.; Linington, R. G.; Tidgewell, K.; Fenner, A. M.; Urena, L. D.; Togna, G. D.; Kyle, D. E.; Gerwick, W. H. *J. Nat. Prod.* **2010**, *73*, 60−66.
(22) Linington, R. G.; Clark, B. R.; Trimble, E. E.; Almanza, A.; Urena, L. D.; Kyle, D. E.; Gerwick, W. H. *J. Nat. Prod.* **2009**, *72*, 14−17.
(23) Medina, R. A.; Goeger, D. E.; Hills, P.; Mooberry, S. L.; Huang, N.; Romero, L. I.; Ortega-Barria, E.; Gerwick, W. H.; McPhail, K. L. *J. Am. Chem. Soc.* **2008**, *130*, 6324−6325.
(24) Choi, H.; Pereira, A. R.; Cao, Z.; Shuman, C. F.; Engene, N.; Byrum, T.; Matainaho, T.; Murray, T. F.; Mangoni, A.; Gerwick, W. H. *J. Nat. Prod.* **2010**, *73*, 1411−1421.
(25) Luesch, H.; Moore, R. E.; Paul, V. J.; Mooberry, S. L.; Corbett, T. H. *J. Nat. Prod.* **2001**, *64*, 907−910.
(26) Pina, I. C.; Gautschi, J. T.; Wang, G. Y.; Sanders, M. L.; Schmitz, F. J.; France, D.; Cornell-Kennon, S.; Sambucetti, L. C.; Remiszewski, S. W.; Perez, L. B.; Bair, K. W.; Crews, P. *J. Org. Chem.* **2003**, *68*, 3866−3873.
(27) Sitachitta, N.; Gerwick, W. H. *J. Nat. Prod.* **1998**, *61*, 681−684.
(28) Maligres, P. E.; Houpis, I.; Rossen, K.; Molina, A.; Sager, J.; Upadhyay, V.; Wells, K. M.; Reamer, R. A.; Lynch, J. E.; Askin, D.; Volante, R. P.; Reider, P. J.; Houghton, P. *Tetrahedron* **1997**, *53*, 10983−10992.
(29) Chen, X.; Wang, L.; Du, Y.; Wu, Y.; Jia, X.; Yang, Y.; Hong, B. *Molecules* **2011**, *16*, 9178−9193.
(30) Castenholz, R. W., Ed. *Bergey's Manual of Systematic Bacteriology*, 2nd ed.; Springer: New York, 2001.
(31) Komárek, J.; Anagnostidis, K. In *Süßwasserflora von Mitteleuropa*; Büdel, B.; Gärtner, G.; Krienitz, L.; Schagerl, M., Eds.; Gustav Fischer: Jena, Germany, 2005; Vol. *19/2*.
(32) Nubel, U.; Garcia-Pichel, F.; Muyzer, G. *Appl. Environ. Microbiol.* **1997**, *63*, 3327−3332.
(33) Katoh, K.; Toh, H. *BMC Bioinformat.* **2008**, *9*, 212.
(34) Cannone, J. J.; Subramanian, S.; Schnare, M. N.; Collett, J. R.; D'Souza, L. M.; Du, Y.; Feng, B.; Lin, N.; Madabusi, L. V.; Muller, K. M.; Pande, N.; Shang, Z.; Yu, N.; Gutell, R. R. *BMC Bioinformat.* **2002**, *3*, 2.
(35) Posada, D. *Mol. Biol. Evol.* **2008**, *25*, 1253−1256.
(36) Guindon, S.; Gascuel, O. *Syst. Biol.* **2003**, *52*, 696−704.
(37) Ronquist, F.; Huelsenbeck, J. P. *Bioinformatics* **2003**, *19*, 1572−1574.
(38) Corbett, Y.; Herrera, L.; Gonzalez, J.; Cubilla, L.; Capson, T. L.; Coley, P. D.; Kursar, T. A.; Romero, L. I.; Ortega-Barria, E. *Am. J. Trop. Med. Hyg.* **2004**, *70*, 119−124.
(39) Williams, C.; Espinosa, O. A.; Montenegro, H.; Cubilla, L.; Capson, T. L.; Ortega-Barria, E.; Romero, L. I. *J. Microbiol. Methods* **2003**, *55*, 813−816.
(40) Molinar-Toribio, E.; Gonzalez, J.; Ortega-Barria, E.; Capson, T. L.; Coley, P. D.; Kursar, T. A.; McPhail, K.; Cubilla-Rios, L. *Pharm. Biol.* **2006**, *44*, 550−553.